EUROPEAN ORGANIZATION FOR NUCLEAR RESEARCH

CERN-EP/2001-046
June 28, 2001

Search for Heavy Neutral and Charged Leptons in e^+e^- Annihilation at LEP

The L3 Collaboration

Abstract

A search for exotic unstable neutral and charged heavy leptons as well as for stable charged heavy leptons is performed with the L3 detector at LEP. Sequential, vector and mirror natures of heavy leptons are considered. No evidence for their existence is found and lower limits on their masses are set.

Submitted to *Phys. Lett. B*

Introduction

Many theories beyond the Standard Model of the electro-weak interation [1] predict the existence of new heavy leptons [2] with observable production cross sections and cleanly identifiable final states. Results on this subject obtained at the Z resonance by LEP and SLC experiments are found in Reference 3. Results obtained by the LEP experiments at centre-of-mass energies, $\sqrt{s} = 133-189$ GeV are found in References 4 and 5. Here we report on a search for exotic pair-produced heavy leptons. The data used in this analysis were collected with the L3 detector [6] at LEP during 1999 at $\sqrt{s} = 192-202$ GeV and 2000 at $\sqrt{s} = 200-208$ GeV with a total integrated luminosity 450 pb^{-1}. The results are combined with our earlier data recorded at $\sqrt{s} = 133 - 189$ GeV.

The exotic leptons discussed in this paper may be classified by their $SU(2) \times U(1)$ quantum numbers [2]:

- Sequential leptons: they exist in the simplest extension of the Standard Model where a fourth family with the same quantum numbers is added to the known fermionic spectrum. The indirect limits on existence of these particles can be found in Reference 7.
- Vector leptons: these particles occur in both left-handed and right-handed weak isodoublets. Among others, the E_6 group model [8] predicts them.
- Mirror leptons [9]: these particles have chiral properties which are opposite to those of ordinary leptons, *i.e.* the right-handed components form a weak isodoublet and the left-handed ones are weak isosinglets. Mirror fermions appear in many extensions of the Standard Model and provide a possible way to restore left-right symmetry at the scale of the electroweak symmetry breaking.

Production and decay of exotic leptons

Charged heavy leptons, $\mathrm{L}^{\pm}$, are pair-produced through the s-channel via γ and Z boson exchange, while for heavy neutral leptons, L^0, only the Z boson exchange is present. The total cross sections are in the range of 1–3 pb at masses well below the beam energy, E_{beam}, and fall as the mass of the lepton approaches the beam energy. The neutral heavy leptons are either of Dirac or Majorana types. The main difference between pair-produced Dirac and Majorana neutral heavy leptons is the dependence of the cross section on their velocity β. A $\beta(3-\beta^2)$ term is present in the Dirac case while the cross section in the Majorana case is proportional to β^3. This implies that the Majorana cross section falls more rapidly with mass than the Dirac one. In this search, heavy leptons couple to the electron, muon, or tau families. Only the case where both heavy leptons decay into the same light lepton family is considered.

Exotic leptons decay via the charged or neutral weak currents through the mixing with a light lepton, except for sequential leptons, which decay only through charged current:

$$\mathrm{L}^{\pm} \rightarrow \nu_{\ell}\mathrm{W}^{\pm} \text{ or } \mathrm{L}^{\pm} \rightarrow \ell^{\pm}\mathrm{Z}$$

$$\mathrm{L}^{0} \rightarrow \ell^{\pm}\mathrm{W}^{\mp} \text{ or } \mathrm{L}^{0} \rightarrow \nu_{\ell}\mathrm{Z}$$

where $\ell = \mathrm{e}, \mu, \tau$. For masses, m_{L}, below 100 GeV, heavy leptons decay predominantly through the W boson. The branching fraction of $\mathrm{L}^0 \rightarrow \mathrm{eW}$ is about 90% for $m_{\mathrm{L}} = 100$ GeV and 100% for $m_{\mathrm{L}} \leq 90$ GeV. Therefore, only the decay into the W boson is considered.

The decay amplitude of $L^0 \to \ell^\pm W^\mp$ contains a mixing parameter U. The mean decay length, D, as a function of $|U|^2$ and mass is given by $D = \beta\gamma c\tau_L \propto \beta|U|^{-2}m_L^\alpha$ [11], where τ_L is the lifetime of the heavy lepton and $\alpha \approx -6$. This implies the decay can occur far from the interaction point if the particle has a low mass or a very small coupling. To ensure high detection and reconstruction efficiencies, this search is restricted to decay lengths below 1cm, which limits the sensitivity to the mixing parameter to $|U|^2 > \mathcal{O}(10^{-11})$.

Two additional possibilities for the charged heavy lepton decays are considered:

- The charged leptons decay through a weak charged current interaction that conserves lepton number, $L^\pm \to L^0 W^\pm$.
- The charged leptons are stable. This is the case if the associated neutral lepton is heavier than its charged partner and the coupling with light leptons is negligible.

Event simulation

The generation of heavy leptons and their decay is performed with the TIPTOP [12] Monte Carlo program which takes into account initial state radiation and spin effects. A mass range between 50 and 100 GeV for the heavy leptons is considered. For the simulation of background from Standard Model processes the following Monte Carlo programs are used: KK2f [13] ($e^+e^- \to q\bar{q}(\gamma)$), PYTHIA [14] ($Ze^+e^-$, ZZ), BHWIDE [15] ($e^+e^- \to e^+e^-(\gamma)$), KORALZ [16] ($e^+e^- \to \mu^+\mu^-(\gamma)$ and $e^+e^- \to \tau^+\tau^-(\gamma)$), KORALW [17] ($e^+e^- \to W^+W^-$), PHOJET [18] ($e^+e^- \to e^+e^-q\bar{q}$), DIAG36 [19] ($e^+e^- \to e^+e^-\ell^+\ell^-$), and EXCALIBUR [20] for other four-fermion final states. The Monte Carlo events are simulated in the L3 detector using the GEANT3 program [21], which takes into account the effects of energy loss, multiple scattering and showering in the materials. Time dependent detector inefficiencies, as monitored during the data taking period, are also simulated.

Search for unstable heavy leptons

Lepton and jet identification

Unstable heavy lepton signatures are characterized by hadronic jets, isolated leptons, and missing energy and transverse momentum.

An electron is identified as a cluster in the electromagnetic calorimeter with an energy larger than 4 GeV matched to a track in the (R, ϕ) plane to within 20 mrad. The cluster profile should be consistent with that expected for an electron. The polar angle of the electron candidate must satisfy $|\cos\theta| < 0.94$. A muon track is required to have track segments in at least two out of three layers of muon chambers and to point back to the interaction region. The muon should have a momentum greater than 4 GeV and a polar angle defined by $|\cos\theta| < 0.8$. The lepton is isolated if less than 5 GeV is deposited in a 30° cone around its direction. Moreover, to eliminate photon conversions, only one matched track is required for isolated electrons. Jets are reconstructed from electromagnetic and hadronic calorimeter clusters using the Durham algorithm [22] with a jet resolution parameter $y_{cut} = 0.008$. The jet momenta are defined by the vectorial energy sum of calorimetric clusters.

The most important backgrounds are W^+W^-, $q\bar{q}(\gamma)$ and ZZ production. The W^+W^- process is rejected by cuts on visible mass, number of hadronic jets, jet angles and energies and lepton energies. The $q\bar{q}(\gamma)$ process is suppressed by demanding transverse momentum imbalance, no energy in the very forward-backward regions, and a missing momentum vector pointing into the detector. For ZZ event rejection, a cut on the energy sum of the two isolated leptons is applied.

Search for unstable neutral heavy leptons

The search for pair-produced neutral heavy leptons requires two isolated leptons (e, μ, or τ) of the same family together with the decay products of W bosons, *i.e.* $e^+e^- \to L^0\overline{L}^0 \to \ell^+\ell^-W^+W^-$. Hadronic events with visible energy greater than 60 GeV and charged track multiplicity greater than 3 are considered.

For the case where both neutral heavy leptons decay to either electrons or muons, events must also satisfy the following criteria:

- The number of reconstructed jets plus isolated leptons is at least 3.
- The event contains at least two isolated electrons or two isolated muons. Figure 1 shows the energy in a 30° cone for the second most energetic electron candidate.
- The energy sum of the two isolated electrons or muons must be less than $0.7\times E_{beam}$. Figure 2 shows the sum of the energies of two muons.

After this selection, 11 events remain in the data for the electron decay mode while 10.7 ± 0.5 background events are expected. For the muon decay mode, 5 events remain in the data while 2.3 ± 0.2 background events are expected.

For the case where both neutral heavy leptons decay to tau leptons, each of the taus decays independently into hadrons, muons, or electrons. When both tau leptons decay into either muons or electrons, the above selection is applied with the exception that we allow the isolated leptons to be either two electrons, two muons, or one muon and one electron. For the case in which at least one of the tau decays into one charged hadron, events are required to satisfy the the following criteria:

- The number of reconstructed jets plus isolated leptons is at least 4.
- The polar angle of the missing momentum must be in the range $25° < \theta_{miss} < 155°$, as depicted in Figure 3, and the fraction of the visible energy in the forward-backward region, $\theta < 20°$ and $\theta > 160°$, must be less than 40%.
- The angle between the most isolated track and the track nearest to it must be greater than 50°, or the angle between the second most isolated track and the track nearest to it must be greater than 25°. The transverse momenta of the two most isolated tracks must be greater than 1.2 GeV, and at least one track must have a transverse momentum greater than 2.5 GeV.
- The electron and muon energies must be less than 50 GeV.

After applying the above selection and also accounting for the case where both taus decay into electrons or muons, 114 events remain in the data, while 121.5 ± 1.6 background events are expected.

Search for unstable charged heavy leptons

Decay into a light neutrino, $\mathrm{L}^{\pm} \rightarrow \nu_{\ell}\mathrm{W}^{\pm}$

For this search, two sets of cuts are used to identify the topology with one hadronic and one leptonic W-decay as well as two hadronic W-decays. For both selections, the visible energy is required to be greater than 50 GeV, the multiplicity of charged tracks to be greater than 3, and the fraction of the total visible energy in the forward-backward region to be less than 25%.

For the decay $\mathrm{L}^{+}\mathrm{L}^{-} \rightarrow \nu_{\ell}\bar{\nu}_{\ell}\ \mathrm{W}^{+}\mathrm{W}^{-} \rightarrow \nu_{\ell}\bar{\nu}_{\ell}\ell\nu_{\ell}\mathrm{q}\bar{\mathrm{q}}'$, events satisfying the following criteria are selected:

- The event contains at least one isolated electron or muon with energy greater than 15 GeV and less than 60 GeV.
- The number of reconstructed jets plus isolated leptons is at least 3.
- The polar angle of the missing momentum must be in the range $25° < \theta_{miss} < 155°$.
- The sum of the energies of the hadronic jets must be less than $0.85 \times E_{beam}$. Figure 4a shows the distribution of the sum of the energies of hadronic jets.

After applying the selection, 76 events remain in the data while 73.1 ± 1.4 background events are expected.

For the mode where both W bosons decay hadronically, events satisfying the following criteria are selected:

- The event does not contain any isolated electron or muon and the energy of each non-isolated electron or muon must be less than 30 GeV.
- The number of hadronic jets is at least 4.

After application of the previous cuts, the dominant remaining background is W-pair production. However, for the signal events, the total visible energy is less than $\sqrt{s}$ and the two W bosons are not back-to-back due to the energy and momentum carried away by light neutrinos. The following additional requirements are then imposed:

- The visible energy must be less than $0.9 \times \sqrt{s}$, as shown in Figure 4b.
- The acollinearity angle between the two W candidates is greater than 15°, as shown in Figure 4c.
- The total transverse momentum of jets must be greater than 10 GeV, as shown in Figure 4d.

For charged heavy lepton masses greater than the W boson mass, the leptons decay to a real W. Therefore, for the case where the charged lepton mass is greater than 80 GeV, a kinematic fit is applied to improve the determination of jet energies and angles. Both jet-jet invariant masses are constrained to the W mass. All possible jet-jet combinations are considered and the one which yields the smallest χ^2 of the fit is chosen.

After applying the selection, 79 events remain in the data while 75.0 ± 1.5 background events are expected.

Decay into a stable neutral heavy lepton, $L^\pm \rightarrow L^0 W^\pm$

The search for a charged heavy lepton decaying into a stable neutral heavy lepton assumes a mass of the associated heavy neutrino L^0 to be greater than 40 GeV. This assumption is based on LEP results at the Z resonance [3] and implies a large missing energy and large transverse momentum imbalance. In the limit of a vanishing mass difference between the charged lepton and its associated neutral lepton, $\Delta m = m_{L^\pm} - m_{L^0}$, the signal efficiency is affected by the trigger efficiency and the rejection of the two-photon background. Here the search is restricted to 5 GeV $\leq \Delta m \leq$ 60 GeV. The case of a light neutrino, $\Delta m = m_{L^\pm}$, is considered in the previous section. The main background is the two-photon process for small mass differences, $\Delta m \leq$ 20 GeVand the $q\bar{q}(\gamma)$ and W^+W^- processes for high mass differences, $\Delta m \geq$ 20 GeV.

This signature is very similar to that of a chargino decaying into a stable neutralino and a W boson. Therefore, a selection developed for the chargino search [23] is used. It is based on the signatures of missing energy, transverse momentum imbalance and isolated leptons. Cuts on missing mass and acoplanarity are also used. The selection is optimized for three different Δm regions: for very low Δm region around 5 GeV, the low Δm range from 10 to 30 GeV and the medium Δm range from 40 to 70 GeV.

After applying the above three selections, 169 events are left in the data while 180.1 ± 6.3 events are expected from background.

Search for stable charged heavy leptons

The analysis follows closely the procedure described in References 4 and 24 and extends the search to higher masses. The signal events are characterized by two back-to-back high momentum tracks in the central tracking detector. Events satisfying the following criteria are selected:

- The event contains two charged tracks, each with momentum greater than 5 GeV and polar angle $|\cos\theta| < 0.82$.
- The acollinearity angle between the two tracks is less than 15^o.

The momentum and acollinearity angle cuts reduce the background from two-photon produced lepton pairs as well as from dilepton annihilation events with a high energy photon in the final state. 16,598 events are selected in the data samples with 16,715 events expected from Standard Model processes, mainly from $e^+e^- \rightarrow e^+e^-$.

Stable charged heavy leptons are also expected to be highly ionizing in the tracking chamber. The dE/dx measurement is calibrated with Bhabha scattering events, and the mean value of the dE/dx distribution is normalized to one. Its resolution is 0.08 units. The ionization energy loss has been studied using low energy protons and kaons in our hadronic events up to 10 units in dE/dx which corresponds to $m_L/E_{beam} = 0.995$. Figure 5 shows the dE/dx measurements of the tracks of data events passing the previous cuts, as well as the simulated signal from pair-production of stable charged heavy leptons. We select candidate events for which the ionization energy loss for each track is between 1.25 and 8.0 units and the product of the track ionization losses is larger than 2.0 units. The upper cut at 8 units rejects very highly ionizing particles for which saturation effects may lead to track reconstruction inefficiencies.

Three candidate events satisfy the selection requirements in the data. The candidate events were recorded at beam energies of 97.8 GeV, 102.7 GeVand 103.3 GeVand correspond to pair production of stable charged particles of masses 82.9 ± 1.8 GeV , 86.5 ± 1.8 GeV and 86.2 ± 2.1 GeV, respectively. However, no candidate events are observed that are consistent with a lepton mass larger than 90 GeV.

The background is estimated using a calibration sample taken on the Z resonance during the 1999 and 2000 data taking periods. From the number of two track events from this sample passing all stable heavy lepton selection cuts, the background is estimated to be 4.1 ± 1.8 events for the entire high energy data sample.

Results

No signal for new heavy leptons is observed. The number of selected events and expected backgrounds are in good agreement. The systematic uncertainty, which is mainly due to the uncertainties in the energy calibration, the lepton identification efficiency and purity, and the Monte Carlo statistics, is estimated to be 5% relative. To obtain exclusion limits, the selection efficiency is reduced by the total systematic uncertainty. These results are combined with our earlier L3 data recorded at $\sqrt{s} = 133 - 189$ GeV [4, 24].

The selection efficiencies are determined by Monte Carlo simulation. For unstable neutral heavy leptons in the mass range from 90 to 100 GeV, the efficiency is 32% to 40% for the electron decay mode, and 27% to 35% for the muon decay mode. For the tau decay mode, the selection efficiency ranges from 13% for a heavy lepton mass of 80 GeV to 20% for a mass of 95 GeV. The selection efficiency for unstable charged heavy leptons of mass 100 GeV decaying into light neutrinos is 24%. In the case of the charged lepton decaying into its associated neutral lepton, the selection efficiency is 5% to 40% with increasing mass difference Δm.

The selection efficiency for stable charged heavy leptons is a function of m_{L}/E_{beam} and ranges from 60% to 70% over the range 0.8 to 0.99, including the trigger efficiency. For $m_{\mathrm{L}}/E_{beam} > 0.99$, the efficiency drops due to the upper cut on track ionization.

Taking into account the luminosities, the selection efficiencies and the production cross sections we calculate the 95% confidence level, CL, lower limits on the masses of heavy leptons [25], which are shown in Tables 1 and 2. The limits for vector heavy leptons are higher than for the sequential and mirror ones due to their production cross section. Figure 6 shows the 95% CL exclusion contour in the $m_{\mathrm{L}^\pm} - m_{\mathrm{L}^0}$ mass plane for decays of the charged lepton into its associated neutral lepton. The lower limit on the mass of the charged heavy lepton is shown in Table 2 for a mass difference greater than 15 GeV. These limits include the full LEP data set and improve upon and supersede our previous results.

Acknowledgements

We wish to express our gratitude to the CERN accelerator divisions for the excellent performance of the LEP machine. We acknowledge with appreciation the effort of the engineers, technicians and support staff who have participated in the construction and maintenance of this experiment.

Table 1: 95% CL lower mass limits in GeV for pair-produced neutral heavy leptons.

Decay mode	Model	Dirac	Majorana
$L^0 \rightarrow eW$	Sequential	101.3	89.5
	Vector	102.6	–
	Mirror	100.8	89.5
$L^0 \rightarrow \mu W$	Sequential	101.5	90.7
	Vector	102.7	–
	Mirror	101.0	90.7
$L^0 \rightarrow \tau W$	Sequential	90.3	80.5
	Vector	99.3	–
	Mirror	90.3	80.5

Table 2: 95% CL lower mass limits in GeV for pair-produced charged heavy leptons.

Decay mode	Model	
$L^\pm \rightarrow \nu W$	Sequential	100.8
	Vector	101.2
	Mirror	100.5
$L^\pm \rightarrow L^0 W$	Sequential	101.9
	Vector	102.1
	Mirror	101.9
Stable	Sequential	102.6
	Vector	102.6
	Mirror	102.6

References

[1] S. L. Glashow, Nucl. Phys. **22** (1961) 579;
S. Weinberg, Phys. Rev. Lett. **19** (1967) 1264;
A. Salam, "Weak and Electromagnetic Interactions", in *Elementary Particle Theory*, edited by N. Svartholm, page 367, Stockholm, 1968, Almqvist and Wiksell.

[2] For a review see:
D. London, in *Precision Tests of the Standard Model*, ed. P. Langacker, World Scientific, Singapore (1995);
A. Djouadi, J. Ng and T.G. Rizzo, in *Electroweak Symmetry Breaking and New Physics at the TeV Scale*, eds. T. Barklow *et al.*, World Scientific, Singapore (1997).

[3] ALEPH Collaboration, D. Decamp *et al.*, Phys. Rep. **216** (1992) 253;
DELPHI Collaboration, P. Abreu *et al.*, Phys. Lett. **B 274** (1992) 230;
L3 Collaboration, O. Adriani *et al.*, Phys. Rep. **236** (1993) 1;
OPAL Collaboration, M.Z. Akrawy *et al.*, Phys. Lett. **B 240** (1990) 250;
OPAL Collaboration, M.Z. Akrawy *et al.*, Phys. Lett. **B 247** (1990) 448;
OPAL Collaboration, M.Z. Akrawy *et al.*, Phys. Lett. **B 252** (1990) 290;

MARK II Collaboration, G.S. Abrams *et al.*, Phys. Rev. Lett. **63** (1989) 2447;
MARK II Collaboration, E. Soderstrom *et al.*, Phys. Rev. Lett. **64** (1990) 2980.

[4] L3 Collaboration, M. Acciarri *et al.*, Phys. Lett. **B 462** (1999) 354.

[5] ALEPH Collaboration, D. Buskulic *et al.*, Phys. Lett. **B 384** (1996) 439;
ALEPH Collaboration, R. Barate *et al.*, Phys. Lett. **B 405** (1997) 379;
DELPHI Collaboration, P. Abreu *et al.*, Eur. Phys. J. **C 8** (1999) 41;
DELPHI Collaboration, P. Abreu *et al.*, Phys. Lett. **B 478** (2000) 65;
OPAL Collaboration, K. Ackerstaff *et al.*, Phys. Lett. **B 433** (1998) 195;
OPAL Collaboration, K. Ackerstaff *et al.*, Eur. Phys. J. **C 14** (2000) 73.

[6] L3 Collaboration, B. Adeva *et al.*, Nucl. Instr. Meth. **A 289** (1990) 35;
M. Acciarri *et al.*, Nucl. Instr. Meth. **A 351** (1994) 300;
M. Chemarin *et al.*, Nucl. Instr. Meth. **A 349** (1994) 345;
M. Adam *et al.*, Nucl. Instr. Meth. **A 383** (1996) 342;
G. Basti *et al.*, Nucl. Instr. Meth. **A 374** (1996) 293.

[7] N. Evans, Phys. Lett. **B 340** (1994) 81;
P. Bamert and C.P. Burgess, Z. Phys. **C 66** (1995) 495;
T. Inami *et al.*, Mod. Phys. Lett. **A 10** (1995) 1471;
A. Masiero *et al.*, Phys. Lett. **B 355** (1995) 329;
V. A. Novikov, *et al.*, Mod. Phys. Lett. **A 10** (1995) 1915; Erratum - ibid. **A 11** (1996) 698;
The Particle Data Group, C. Caso *et al.*, Eur. Phys. J. **C 3** (2000) 95.

[8] For a review, see J. Hewett and T.G. Rizzo, Phys. Rep. **183**, (1989) 193.

[9] M. Maalampi and M. Roos, Phys. Rep. **186** (1990) 53.

[10] S.L. Glashow, J. Iliopoulos and L. Maiani, Phys. Rev. **D 2** (1970) 1285.

[11] M. Gronau, C. Leung and J. Rosner, Phys. Rev. **D 29** (1984) 2539.

[12] S. Jadach and J. Kühn, TIPTOP Monte Carlo, Preprint MPI-PAE/PTh 64/86.

[13] KK2F version 4.12 is used: S. Jadach, B.F.L. Ward and Z. Wąs, Comp. Phys. Comm. **130** (2000) 260.

[14] PYTHIA version 5.772 and JETSET version 7.409 are used: T. Sjöstrand, Comp. Phys. Comm. **82** (1994) 74.

[15] BHWIDE version 1.01 is used: S. Jadach *et al.*, Phys. Lett. **D 390** (1997) 298.

[16] KORALZ version 4.02 is used: S. Jadach, J. Kühn and Z. Wąs, Comp. Phys. Comm. **64** (1991) 275;
S. Jadach, B.F.L.Ward and Z. Wąs, Comp. Phys. Comm. **66** (1991) 367.

[17] KORALW version 1.33 is used: S. Jadach *et al.,* Comp. Phys. Comm. **94** (1996) 216;
S. Jadach *et al.,* Phys. Lett. **B 372** (1996) 289.

[18] PHOJET version 1.05 is used: R. Engel, Z. Phys. **C 66** (1993) 1657;
R. Engel and J. Ranft, Phys. Rev. **D 54** (1996) 4244.

[19] F.A. Berends, P.H. Daverveldt and R. Kleiss, Nucl. Phys. **B 253** (1985) 441.

[20] F.A. Berends, R. Kleiss and R. Pittau, Comp. Phys. Comm. **85** (1995) 437.

[21] R. Brun et al., GEANT 3.15 preprint CERN DD/EE/84-1 (1984), revised 1987; H. Fesefeldt, RWTH Aachen report PITHA 85/2 (1985).

[22] S. Catani *et al.*, Phys. Lett. **B 269** (1991) 432;
S. Bethke *et al.*, Nucl. Phys. **B 370** (1992) 310.

[23] L3 Collab., M. Acciarri *et al.*, Phys. Lett. **472** (2000) 420.

[24] L3 Collab., M. Acciarri *et al.*, Phys. Lett. **462** (1999) 354.

[25] V.F. Obraztsov, Nucl. Instr. Meth. **A 316** (1992) 388.

The L3 Collaboration:

P.Achard,[20] O.Adriani,[17] M.Aguilar-Benitez,[24] J.Alcaraz,[24,18] G.Alemanni,[22] J.Allaby,[18] A.Aloisio,[28] M.G.Alviggi,[28]
H.Anderhub,[47] V.P.Andreev,[6,33] F.Anselmo,[9] A.Arefiev,[27] T.Azemoon,[3] T.Aziz,[10,18] M.Baarmand,[25] P.Bagnaia,[38]
A.Bajo,[24] G.Baksay,[16]L.Baksay,[25] S.V.Baldew,[2] S.Banerjee,[10] Sw.Banerjee,[4] A.Barczyk,[47,45] R.Barillère,[18]
P.Bartalini,[22] M.Basile,[9] N.Batalova,[44] R.Battiston,[32] A.Bay,[22] F.Becattini,[17] U.Becker,[14] F.Behner,[47] L.Bellucci,[17]
R.Berbeco,[3] J.Berdugo,[24] P.Berges,[14] B.Bertucci,[32] B.L.Betev,[47] M.Biasini,[32] A.Biland,[47] J.J.Blaising,[4] S.C.Blyth,[34]
G.J.Bobbink,[2] A.Böhm,[1] L.Boldizsar,[13] B.Borgia,[38] D.Bourilkov,[47] M.Bourquin,[20] S.Braccini,[20] J.G.Branson,[40]
F.Brochu,[4] A.Buijs,[43] J.D.Burger,[14] W.J.Burger,[32] X.D.Cai,[14] M.Capell,[14] G.Cara Romeo,[9] G.Carlino,[28] A.Cartacci,[17]
J.Casaus,[24] F.Cavallari,[38] N.Cavallo,[35] C.Cecchi,[32] M.Cerrada,[24] M.Chamizo,[20] Y.H.Chang,[49] M.Chemarin,[23]
A.Chen,[49] G.Chen,[7] G.M.Chen,[7] H.F.Chen,[21] H.S.Chen,[7] G.Chiefari,[28] L.Cifarelli,[39] F.Cindolo,[9] I.Clare,[14] R.Clare,[37]
G.Coignet,[4] N.Colino,[24] S.Costantini,[38] B.de la Cruz,[24] S.Cucciarelli,[32] T.S.Dai,[14] J.A.van Dalen,[30] R.de Asmundis,[28]
P.Déglon,[20] J.Debreczeni,[13] A.Degré,[4] K.Deiters,[45] D.della Volpe,[28] E.Delmeire,[20] P.Denes,[36] F.DeNotaristefani,[38]
A.De Salvo,[47] M.Diemoz,[38] M.Dierckxsens,[2] D.van Dierendonck,[2] C.Dionisi,[38] M.Dittmar,[47,18] A.Doria,[28]
M.T.Dova,[11,♯] D.Duchesneau,[4] P.Duinker,[2] B.Echenard,[20] A.Eline,[18] H.El Mamouni,[23] A.Engler,[34] F.J.Eppling,[14]
A.Ewers,[1] P.Extermann,[20] M.A.Falagan,[24] S.Falciano,[38] A.Favara,[18] J.Fay,[23] O.Fedin,[33] M.Felcini,[47] T.Ferguson,[34]
H.Fesefeldt,[1] E.Fiandrini,[32] J.H.Field,[20] F.Filthaut,[30] P.H.Fisher,[14] W.Fisher,[36] I.Fisk,[40] G.Forconi,[14]
K.Freudenreich,[47] C.Furetta,[26] Yu.Galaktionov,[27,14] S.N.Ganguli,[10] P.Garcia-Abia,[5,18] M.Gataullin,[31] S.Gentile,[38]
S.Giagu,[38] Z.F.Gong,[21] G.Grenier,[23] O.Grimm,[47] M.W.Gruenewald,[8,1] M.Guida,[39] R.van Gulik,[2] V.K.Gupta,[36]
A.Gurtu,[10] L.J.Gutay,[44] D.Haas,[5] D.Hatzifotiadou,[9] T.Hebbeker,[8,1] A.Hervé,[18] J.Hirschfelder,[34] H.Hofer,[47]
G. Holzner,[47] S.R.Hou,[49] Y.Hu,[30] B.N.Jin,[7] L.W.Jones,[3] P.de Jong,[2] I.Josa-Mutuberría,[24] D.Käfer,[1] M.Kaur,[15]
M.N.Kienzle-Focacci,[20] J.K.Kim,[42] J.Kirkby,[18] W.Kittel,[30] A.Klimentov,[14,27] A.C.König,[30] M.Kopal,[44]
V.Koutsenko,[14,27] M.Kräber,[47] R.W.Kraemer,[34] W.Krenz,[1] A.Krüger,[46] A.Kunin,[14,27] P.Ladron de Guevara,[24]
I.Laktineh,[23] G.Landi,[17] M.Lebeau,[18] A.Lebedev,[14] P.Lebrun,[23] P.Lecomte,[47] P.Lecoq,[18] P.Le Coultre,[47] H.J.Lee,[8]
J.M.Le Goff,[18] R.Leiste,[46] P.Levtchenko,[33] C.Li,[21] S.Likhoded,[46] C.H.Lin,[49] W.T.Lin,[49] F.L.Linde,[2] L.Lista,[28]
Z.A.Liu,[7] W.Lohmann,[46] E.Longo,[38] Y.S.Lu,[7] K.Lübelsmeyer,[1] C.Luci,[38] D.Luckey,[14] L.Luminari,[38] W.Lustermann,[47]
W.G.Ma,[21] L.Malgeri,[20] A.Malinin,[27] C.Maña,[24] D.Mangeol,[30] J.Mans,[36] J.P.Martin,[23] F.Marzano,[38] K.Mazumdar,[10]
R.R.McNeil,[6] S.Mele,[18] L.Merola,[28] M.Meschini,[17] W.J.Metzger,[30] A.Mihul,[12] H.Milcent,[18] G.Mirabelli,[38] J.Mnich,[1]
G.B.Mohanty,[10] G.S.Muanza,[23] A.J.M.Muijs,[2] B.Musicar,[40] M.Musy,[38] S.Nagy,[16] M.Napolitano,[28] F.Nessi-Tedaldi,[47]
H.Newman,[31] T.Niessen,[1] A.Nisati,[38] H.Nowak,[46] R.Ofierzynski,[47] G.Organtini,[38] C.Palomares,[18] D.Pandoulas,[1]
P.Paolucci,[28] R.Paramatti,[38] G.Passaleva,[17] S.Patricelli,[28] T.Paul,[11] M.Pauluzzi,[32] C.Paus,[14] F.Pauss,[47] M.Pedace,[38]
S.Pensotti,[26] D.Perret-Gallix,[4] B.Petersen,[30] D.Piccolo,[28] F.Pierella,[9] P.A.Piroué,[36] E.Pistolesi,[26] V.Plyaskin,[27]
M.Pohl,[20] V.Pojidaev,[17] H.Postema,[14] J.Pothier,[18] D.O.Prokofiev,[44] D.Prokofiev,[33] J.Quartieri,[39] G.Rahal-Callot,[47]
M.A.Rahaman,[10] P.Raics,[16] N.Raja,[10] R.Ramelli,[47] P.G.Rancoita,[26] R.Ranieri,[17] A.Raspereza,[46] P.Razis,[29]D.Ren,[47]
M.Rescigno,[38] S.Reucroft,[11] S.Riemann,[46] K.Riles,[3] B.P.Roe,[3] L.Romero,[24] A.Rosca,[8] S.Rosier-Lees,[4] S.Roth,[1]
C.Rosenbleck,[1] B.Roux,[30] J.A.Rubio,[18] G.Ruggiero,[17] H.Rykaczewski,[47] A.Sakharov,[47] S.Saremi,[6] S.Sarkar,[38]
J.Salicio,[18] E.Sanchez,[24] M.P.Sanders,[30] C.Schäfer,[18] V.Schegelsky,[33] S.Schmidt-Kaerst,[1] D.Schmitz,[1] H.Schopper,[48]
D.J.Schotanus,[30] G.Schwering,[1] C.Sciacca,[28] L.Servoli,[32] S.Shevchenko,[31] N.Shivarov,[41] V.Shoutko,[27,14] E.Shumilov,[27]
A.Shvorob,[31] T.Siedenburg,[1] D.Son,[42] P.Spillantini,[17] M.Steuer,[14] D.P.Stickland,[36] B.Stoyanov,[41] A.Straessner,[18]
K.Sudhakar,[10] G.Sultanov,[41] L.Z.Sun,[21] S.Sushkov,[8] H.Suter,[47] J.D.Swain,[11] Z.Szillasi,[25,¶] X.W.Tang,[7] P.Tarjan,[16]
L.Tauscher,[5] L.Taylor,[11] B.Tellili,[23] D.Teyssier,[23] C.Timmermans,[30] Samuel C.C.Ting,[14] S.M.Ting,[14] S.C.Tonwar,[10,18]
J.Tóth,[13] C.Tully,[36] K.L.Tung,[7]Y.Uchida,[14] J.Ulbricht,[47] E.Valente,[38] V.Veszpremi,[25] G.Vesztergombi,[13] I.Vetlitsky,[27]
D.Vicinanza,[39] G.Viertel,[47] S.Villa,[37] M.Vivargent,[4] S.Vlachos,[5] I.Vodopianov,[33] H.Vogel,[34] H.Vogt,[46] I.Vorobiev,[3427]
A.A.Vorobyov,[33] M.Wadhwa,[5] R.T.van de Walle,[30] W.Wallraff,[1] M.Wang,[14] X.L.Wang,[21] Z.M.Wang,[21] M.Weber,[1]
P.Wienemann,[1] H.Wilkens,[30] S.X.Wu,[14] S.Wynhoff,[18] L.Xia,[31] Z.Z.Xu,[21] J.Yamamoto,[3] B.Z.Yang,[21] C.G.Yang,[7]
H.J.Yang,[3] M.Yang,[7] S.C.Yeh,[50] An.Zalite,[33] Yu.Zalite,[33] Z.P.Zhang,[21] J.Zhao,[21] G.Y.Zhu,[7] R.Y.Zhu,[31] H.L.Zhuang,[7]
A.Zichichi,[9,18,19] G.Zilizi,[25,¶] B.Zimmermann,[47] M.Zöller.[1]

1 I. Physikalisches Institut, RWTH, D-52056 Aachen, FRG[§]
III. Physikalisches Institut, RWTH, D-52056 Aachen, FRG[§]
2 National Institute for High Energy Physics, NIKHEF, and University of Amsterdam, NL-1009 DB Amsterdam, The Netherlands
3 University of Michigan, Ann Arbor, MI 48109, USA
4 Laboratoire d'Annecy-le-Vieux de Physique des Particules, LAPP,IN2P3-CNRS, BP 110, F-74941 Annecy-le-Vieux CEDEX, France
5 Institute of Physics, University of Basel, CH-4056 Basel, Switzerland
6 Louisiana State University, Baton Rouge, LA 70803, USA
7 Institute of High Energy Physics, IHEP, 100039 Beijing, China[△]
8 Humboldt University, D-10099 Berlin, FRG[§]
9 University of Bologna and INFN-Sezione di Bologna, I-40126 Bologna, Italy
10 Tata Institute of Fundamental Research, Mumbai (Bombay) 400 005, India
11 Northeastern University, Boston, MA 02115, USA
12 Institute of Atomic Physics and University of Bucharest, R-76900 Bucharest, Romania
13 Central Research Institute for Physics of the Hungarian Academy of Sciences, H-1525 Budapest 114, Hungary[‡]
14 Massachusetts Institute of Technology, Cambridge, MA 02139, USA
15 Panjab University, Chandigarh 160 014, India.
16 KLTE-ATOMKI, H-4010 Debrecen, Hungary[¶]
17 INFN Sezione di Firenze and University of Florence, I-50125 Florence, Italy
18 European Laboratory for Particle Physics, CERN, CH-1211 Geneva 23, Switzerland
19 World Laboratory, FBLJA Project, CH-1211 Geneva 23, Switzerland
20 University of Geneva, CH-1211 Geneva 4, Switzerland
21 Chinese University of Science and Technology, USTC, Hefei, Anhui 230 029, China[△]
22 University of Lausanne, CH-1015 Lausanne, Switzerland
23 Institut de Physique Nucléaire de Lyon, IN2P3-CNRS,Université Claude Bernard, F-69622 Villeurbanne, France
24 Centro de Investigaciones Energéticas, Medioambientales y Tecnologícas, CIEMAT, E-28040 Madrid, Spain♭
25 Florida Institute of Technology, Melbourne, FL 32901, USA
26 INFN-Sezione di Milano, I-20133 Milan, Italy
27 Institute of Theoretical and Experimental Physics, ITEP, Moscow, Russia
28 INFN-Sezione di Napoli and University of Naples, I-80125 Naples, Italy
29 Department of Physics, University of Cyprus, Nicosia, Cyprus
30 University of Nijmegen and NIKHEF, NL-6525 ED Nijmegen, The Netherlands
31 California Institute of Technology, Pasadena, CA 91125, USA
32 INFN-Sezione di Perugia and Università Degli Studi di Perugia, I-06100 Perugia, Italy
33 Nuclear Physics Institute, St. Petersburg, Russia
34 Carnegie Mellon University, Pittsburgh, PA 15213, USA
35 INFN-Sezione di Napoli and University of Potenza, I-85100 Potenza, Italy
36 Princeton University, Princeton, NJ 08544, USA
37 University of Californa, Riverside, CA 92521, USA
38 INFN-Sezione di Roma and University of Rome, "La Sapienza", I-00185 Rome, Italy
39 University and INFN, Salerno, I-84100 Salerno, Italy
40 University of California, San Diego, CA 92093, USA
41 Bulgarian Academy of Sciences, Central Lab. of Mechatronics and Instrumentation, BU-1113 Sofia, Bulgaria
42 The Center for High Energy Physics, Kyungpook National University, 702-701 Taegu, Republic of Korea
43 Utrecht University and NIKHEF, NL-3584 CB Utrecht, The Netherlands
44 Purdue University, West Lafayette, IN 47907, USA
45 Paul Scherrer Institut, PSI, CH-5232 Villigen, Switzerland
46 DESY, D-15738 Zeuthen, FRG
47 Eidgenössische Technische Hochschule, ETH Zürich, CH-8093 Zürich, Switzerland
48 University of Hamburg, D-22761 Hamburg, FRG
49 National Central University, Chung-Li, Taiwan, China
50 Department of Physics, National Tsing Hua University, Taiwan, China

§ Supported by the German Bundesministerium für Bildung, Wissenschaft, Forschung und Technologie
‡ Supported by the Hungarian OTKA fund under contract numbers T019181, F023259 and T024011.
¶ Also supported by the Hungarian OTKA fund under contract number T026178.
♭ Supported also by the Comisión Interministerial de Ciencia y Tecnología.
♯ Also supported by CONICET and Universidad Nacional de La Plata, CC 67, 1900 La Plata, Argentina.
△ Supported by the National Natural Science Foundation of China.

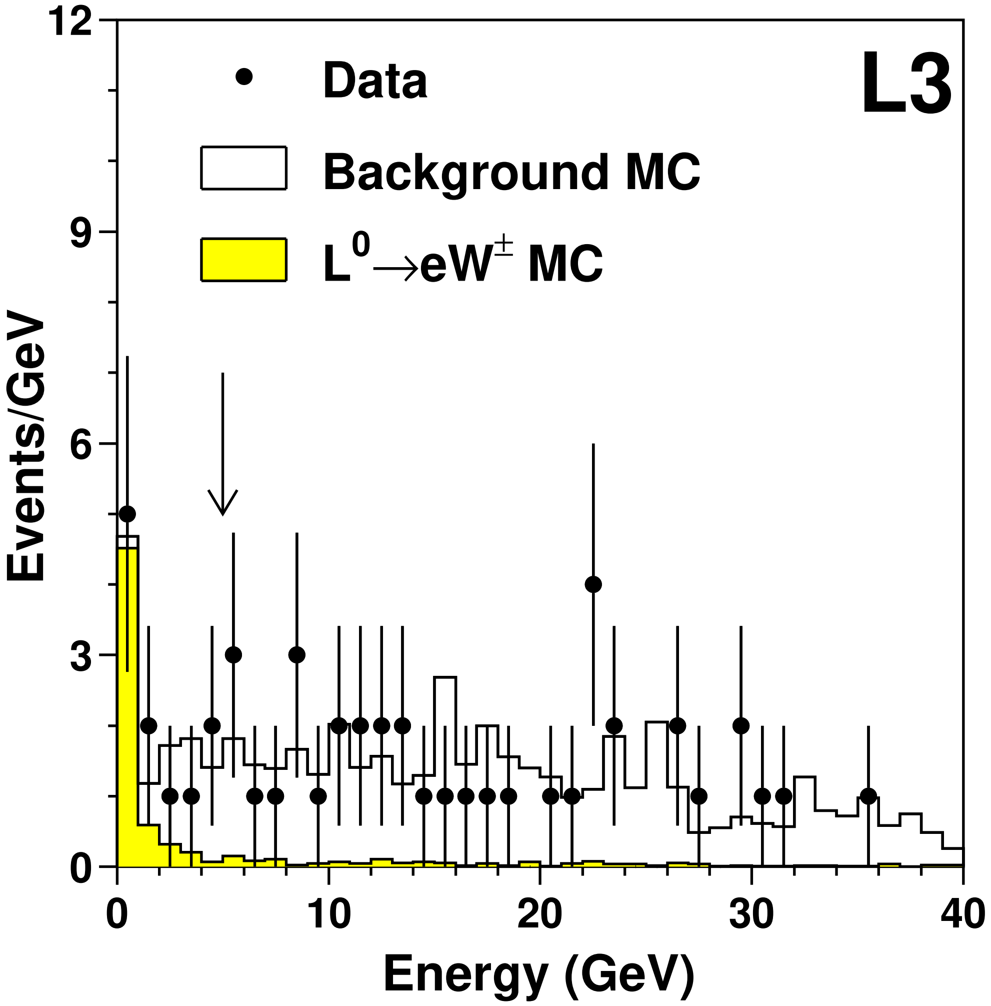

Figure 1: The distribution of the energy in a 30° cone around the second most energetic electron candidate. The points are the data, the solid histogram is the background Monte Carlo. The shaded histogram represents the simulated signal for $e^+e^- \rightarrow L^0\overline{L^0}$ for a sequential Dirac neutral lepton mass of 101 GeV. Both histograms are normalized to the luminosity of the data. The arrow indicates the value of the applied cut; all other selection cuts are applied.

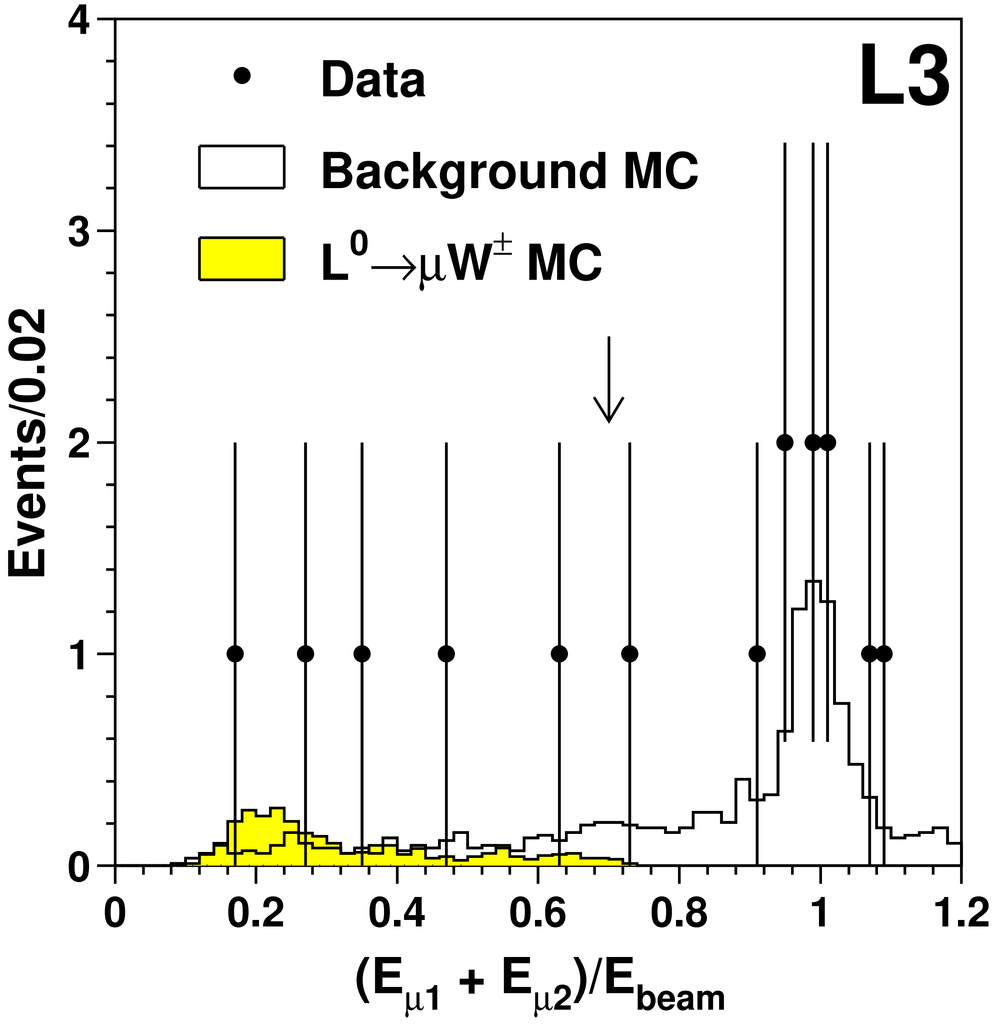

Figure 2: The distribution of the sum of the muon energies, $E_{\mu 1} + E_{\mu 2}$, normalized to the beam enery. The points are the data, the solid histogram is the background Monte Carlo. The shaded histogram represents the simulated signal for $\mathrm{e^+e^-} \to \mathrm{L^0\overline{L^0}}$ for a sequential Dirac neutral lepton mass equal to 101 GeV. Both histograms are normalized to the luminosity of the data. The arrow indicates the value of the applied cut; all other selection cuts are applied.

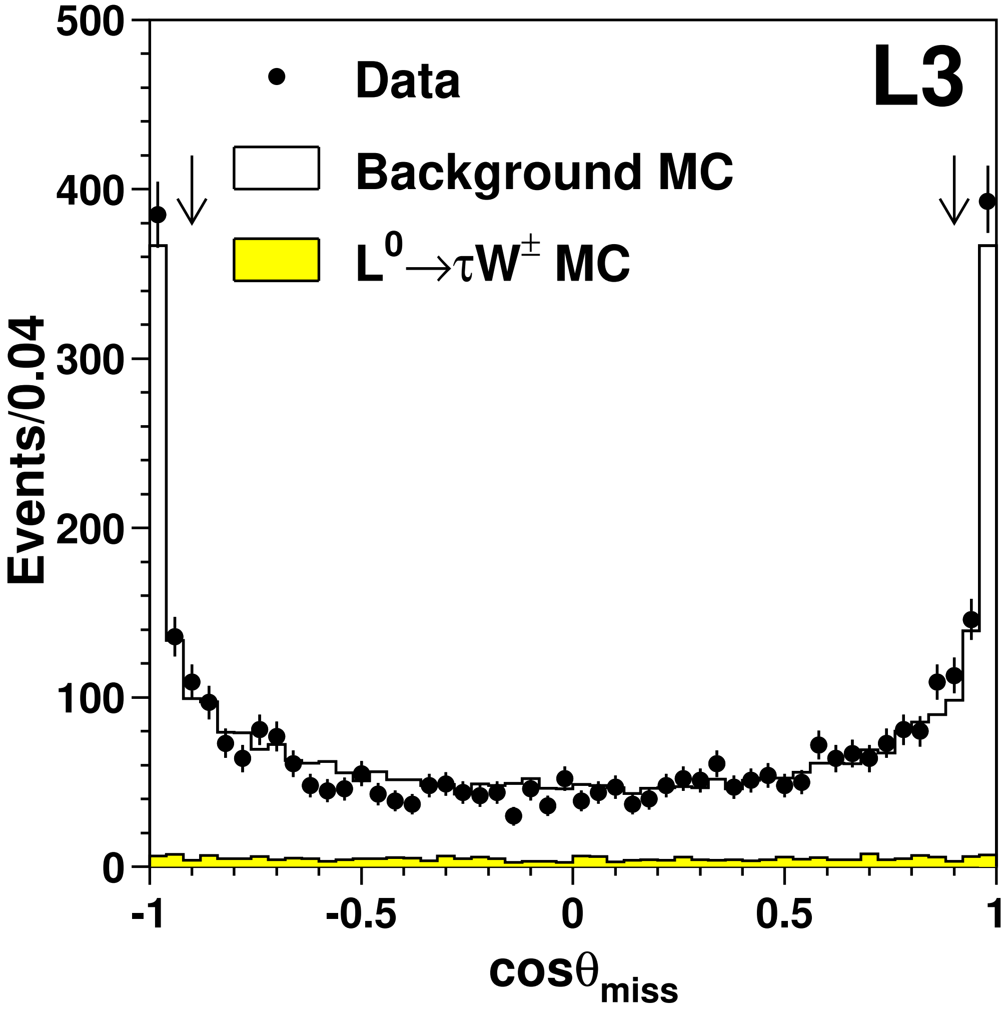

Figure 3: The distribution of the cosine of the polar angle of the missing momentum, $\cos\theta_{miss}$. The points are the data, the solid histogram is the background Monte Carlo. The shaded histogram represents the simulated signal for $e^+e^- \rightarrow L^0\overline{L^0}$ for a sequential Dirac neutral lepton mass equal to 80 GeV. The normalization for the signal Monte Carlo is scaled by a factor of 2 for better visibility. The arrows indicate the values of the applied cut.

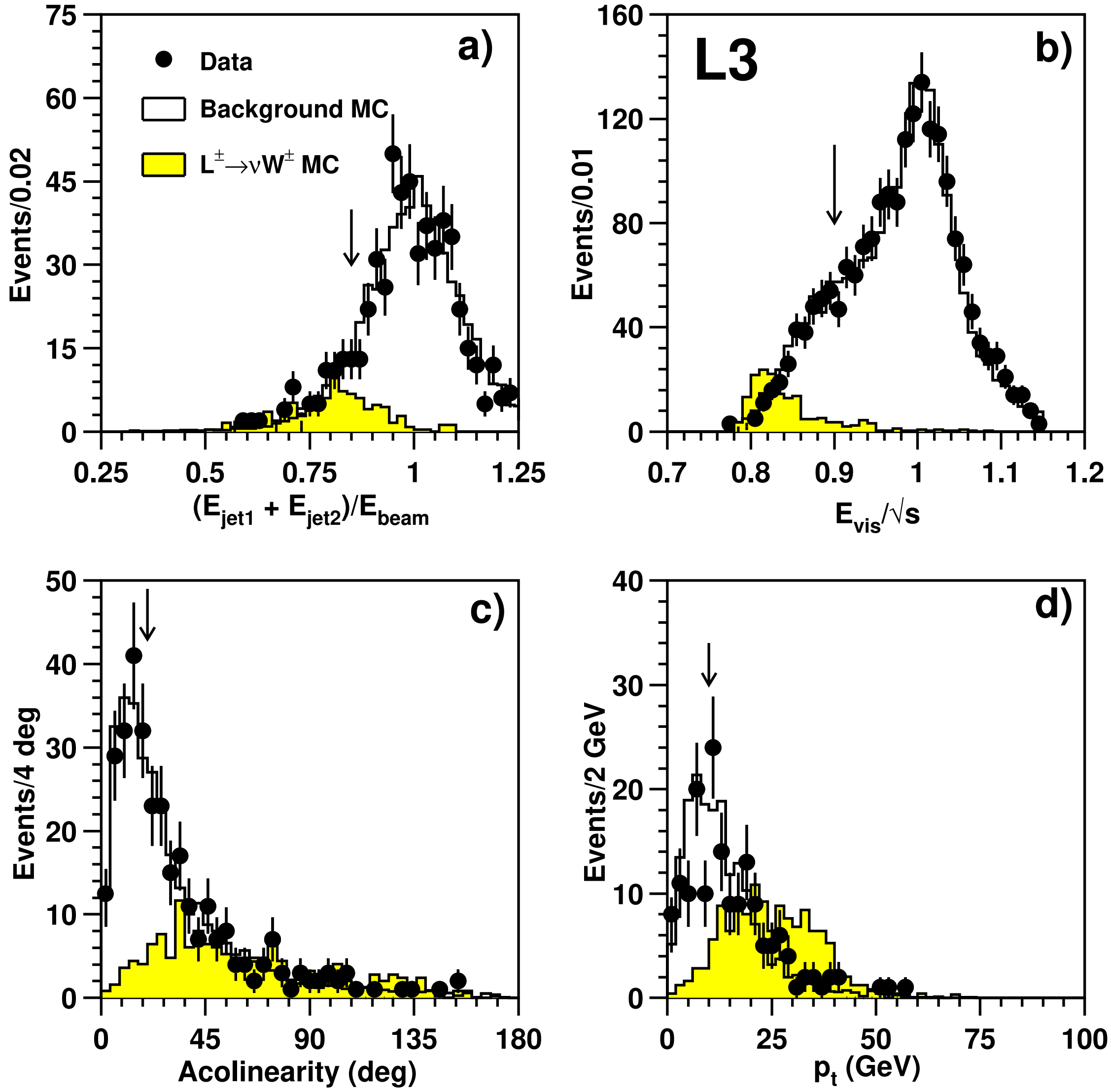

Figure 4: The distribution of a) the sum, $E_{jet_1} + E_{jet_2}$, of the energies of the hadronic jets normalized to the beam energy, b) the normalized visible energy in the event, c) the acollinearity angle of the two W candidates, d) the total transverse momentum, p_t. The points are the data, the solid histogram is the background Monte Carlo. The shaded histogram represents the simulated signal for $e^+e^- \rightarrow L^+L^-$ for a sequential charged lepton mass equal to 95 GeV. The normalization for the signal Monte Carlo is scaled by a factor of 2 for better visibility. The arrows indicate the values of the applied cuts after all the other selection requirements.

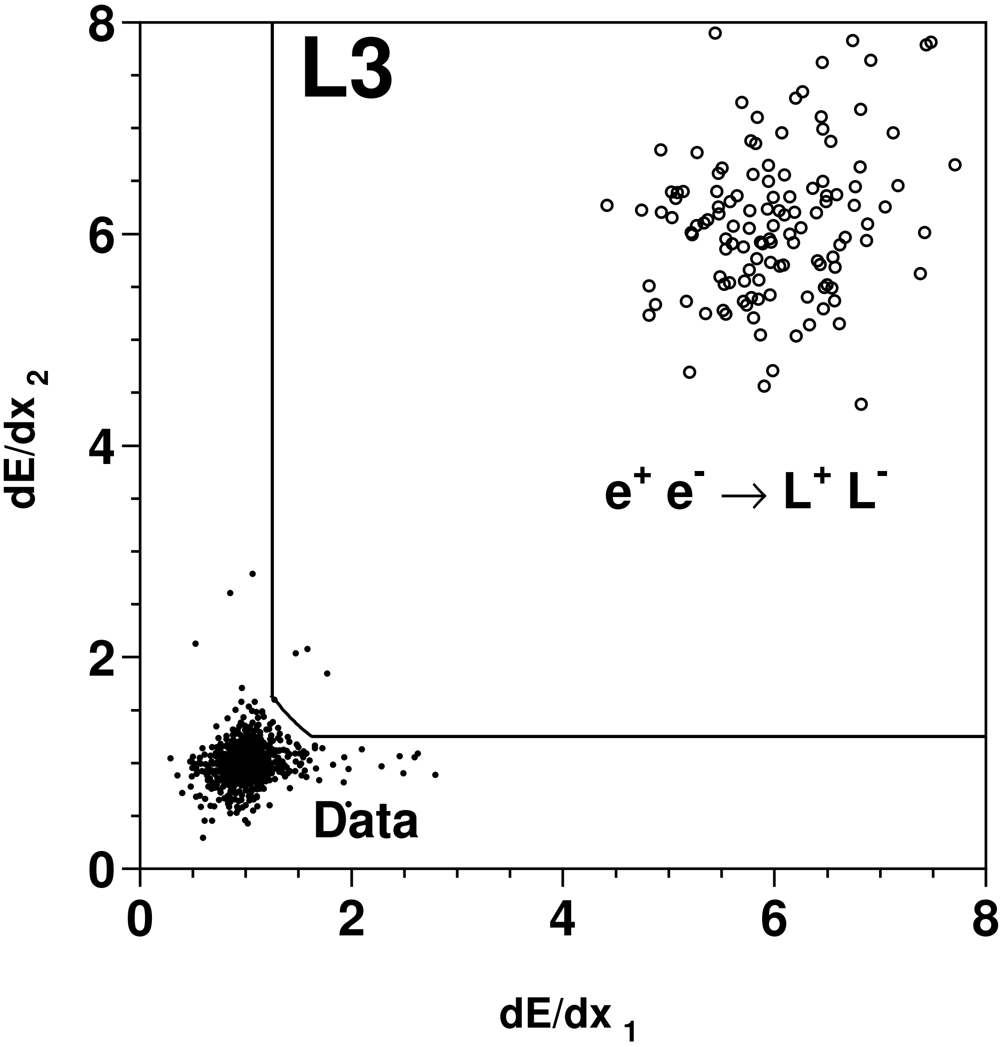

Figure 5: The two dimensional distribution of the ionization energy loss of the most energetic track, dE/dx_1, and the least energetic track, dE/dx_2. The solid circles represent the data and the open circles represent the simulated signal for $e^+e^- \rightarrow L^+L^-$ for a lepton mass of $0.985 \times E_{beam}$. The signal normalization is arbitrary. The lines indicate the values of the applied cut.

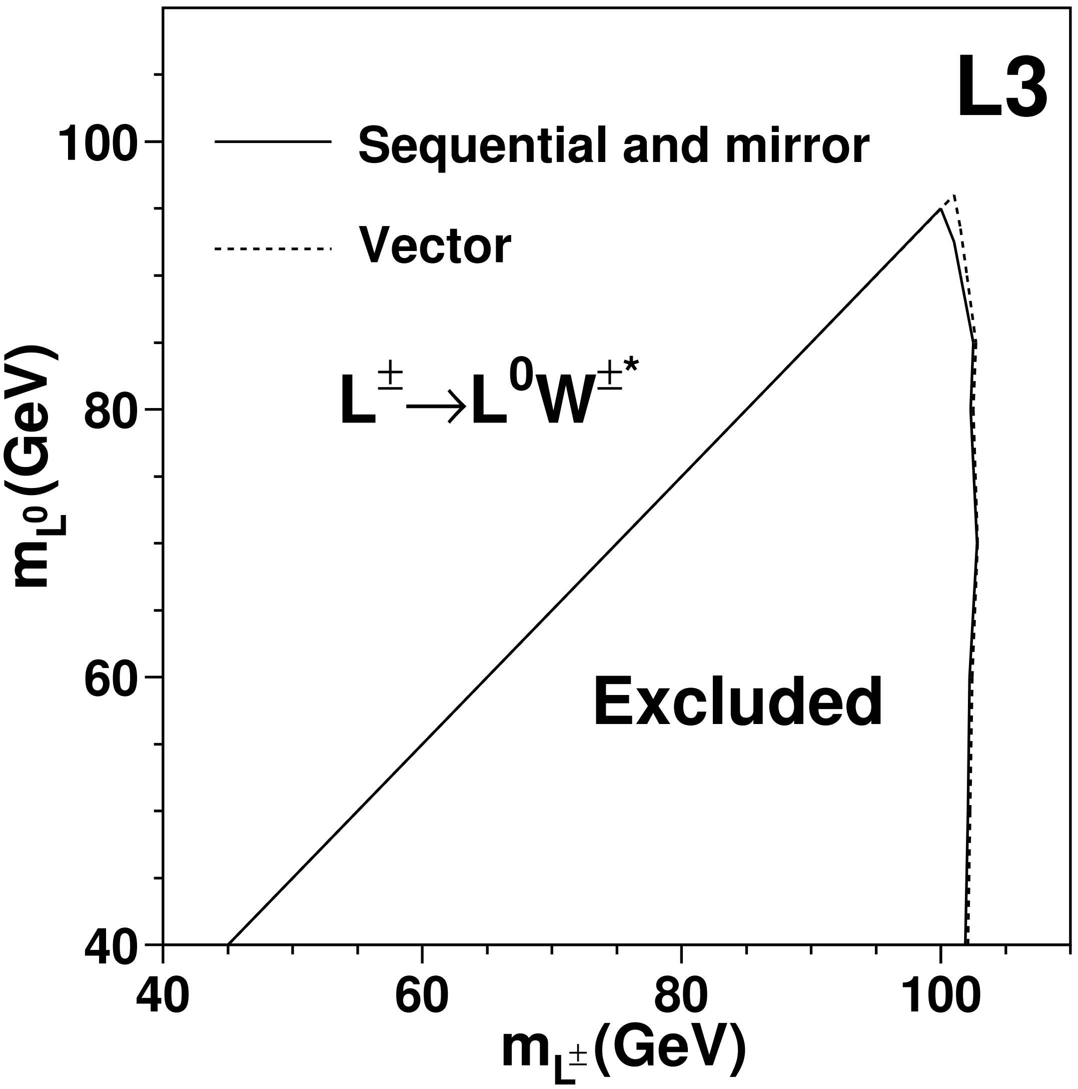

Figure 6: The 95% CL limit in the $m_{\mathrm{L}^\pm} - m_{\mathrm{L}^0}$ plane for the case of a charged heavy lepton decaying into a stable neutral heavy lepton. The solid and dashed lines represent respectively the sequential and mirror, and vector types of heavy lepton.